Journal of Sol-Gel Science and Technology (2024) 111:73–82
https://doi.org/10.1007/s10971-024-06397-7

ORIGINAL PAPER

Investigation of different deposition methods for synthesized gold nanoparticles on a South African sugarcane leaves derived silica xerogel support

Ncamisile Nondumiso Maseko[1] · Dirk Enke[1,2] · Samuel Ayodele Iwarere[3] · Oluwatobi Samuel Oluwafemi[4,5] · Jonathan Pocock[1]

Received: 17 November 2023 / Accepted: 19 April 2024 / Published online: 4 June 2024

Abstract

Value added materials made from agricultural residues are very attractive since they contribute in reducing environmental waste and enhancing economic sustainability. Two deposition methods were investigated where silica xerogel from sugarcane leaves (a waste from sugarcane industry) was used as a support for the synthesized gold nanoparticles. Biogenic silica was refluxed with sodium hydroxide at 80 °C to form sodium silicate solution. The gold nanoparticles were either synthesized in the sodium silicate solution or separately to form silica/Au nanoparticles through a sol-gel method. Ultraviolet (UV)-visible spectroscopy, x-ray powder diffraction (XRD), transmission electron microscopy (TEM), scanning electron microscopy (SEM), x-ray fluorescence spectroscopy (XRF), energy dispersive x-ray (EDX) and nitrogen adsorption-desorption were used to characterize the produced Si/Au nanoparticles. The two investigated methods resulted in distinctive deposition of gold nanoparticles on a silica xerogel support and also significantly different textural properties. The produced silica/gold nanoparticles had a Brunauer-Emmett-Teller (BET) surface area of up to 619 m^2/g, pore diameter of 8.3 nm and pore volume of 1.28 $cm^3.g^{-1}$.

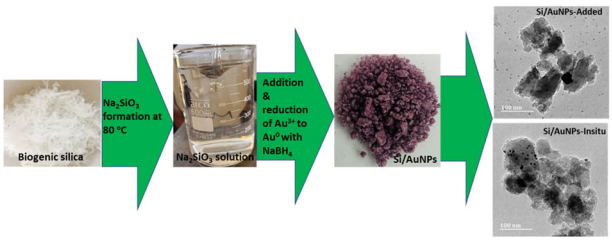

Keywords Silica xerogel · Gold nanoparticles · Amorphous biogenic silica · Sugarcane leaves · In situ synthesis

✉ Ncamisile Nondumiso Maseko
masekon@ukzn.ac.za

[1] Discipline of Chemical Engineering, University of KwaZulu-Natal, 238 Mazisi Kunene Road, Glenwood, Durban 4041, South Africa

[2] Institute of Chemical Technology, Universität Leipzig, Linnéstr. 3, 04103 Leipzig, Germany

[3] Department of Chemical Engineering, University of Pretoria, Lynnwood Road, Hatfield, Pretoria 0028, South Africa

[4] Department of Chemical Sciences (Formerly Applied Chemistry), University of Johannesburg, Doornfontein Campus, P.O. Box 17011, Doornfontein 2028, South Africa

[5] Centre for Nanomaterials Science Research, University of Johannesburg, Johannesburg 2000, South Africa

Highlights

- Sugarcane leaves were used as a source of silica (SiO2) xerogel via a sol-gel method.
- The method of gold nanoparticles (AuNPs) deposition affected the produced Silica/AuNPs.
- Silica /AuNPs synthesized insitu retained a good concentration of Au.
- The synthesized solid SiO_2/AuNPs retained the shape of the gel after drying.
- The deposited AuNPs are spherical in shape but suffered from agglomeration.

1 Introduction

There has been a growing fascination about the design of nanostructured materials and nanoparticles in recent years [1]. As a result, extensive research has been conducted on nanoparticles of noble metals such as silver, gold, palladium and platinum due to their exceptional physicochemical properties and applications in catalysis [2]. Noble metals nanoparticles have high specific surface area which makes it possible for more active sites to be exposed which in turn exhibit a higher catalytic performance [2]. Out of the mentioned noble metal nanoparticles, gold nanoparticles are however the most researched due to the fact that at its nanoscale, gold is the most stable noble metal [1]. The synthesis of gold nanoshells with various dimensions and shapes presents the possibility of acquiring metallic nanoshells that consists of a surface plasmon resonance band located in the near-infrared range [3]. Gold nanoparticles have been reported to be involved in many major chemical transformations such as the oxidation of hydrocarbons and alcohols [4], redox reactions, dehydrogenation and hydrogenation reactions [5]. Other applications of gold nanoparticles are in the field of biomedical imaging, biosensors, fluorescent sensors, photothermal therapy, drug carriers for cancer treatment [3]. According to Min and Friend [6], their catalytic properties are directly affected by particle size and morphology. Generally, the smaller the size of the nanoparticles, the greater their catalytic activity [2].

Gold nanoparticles have a relatively high surface area to volume ratio and in addition are reported to likely stick together to form clusters or larger particles [2, 5]. When it comes to catalytic applications, directly using gold nanoparticles requires a tedious setup procedure to isolate the nanoparticles from the reaction medium or product due to their small sizes and as a result large amounts of waste becomes involved which leads to the manufacturing processes being expensive [7]. In addition, when gold nanoparticles are used directly in catalytic applications, recycling becomes impossible. Deposition of gold nanoparticles on a solid support can efficiently reduce/prevent the nanoparticles from aggregating [2, 5]. As opposed to homogenous catalysts, catalysts on a solid support are often preferred as they are easy to work with [7]. The solid support makes using gold nanoparticles more desirable because it makes it easy to separate from the reaction medium and also enables the option of recycling the catalyst. Different metal oxide supports have been used for the gold nanoparticles but silica materials have been substantially studied due to their nontoxic nature, easy modification and also their insignificant absorption in regions of visible, ultraviolet and near-infrared [8]. Due to their large specific surface area and pore volume, mesoporous silica materials have been utilized in various applications such as drug delivery systems [9], adsorbents [10], biosensors [11] and catalyst supports [12]. Gold nanoparticles have been reported by [2] to have the capability to deposit on the pore surface of biogenic mesoporous silica, they exhibit excellent chemical and thermal stability and also have a high surface area. The resulting silica-gold nanoparticles have attractive properties such as large pore volume, high specific surface area, tunable pore diameter and particle size, good biocompatibility, facile surface for functionalization, and flexible morphology [13]. Due to these unique properties, gold nanoparticles deposited on a silica support have been widely used in adsorption and biomedicine [14–16]. They can be utilized in biomedical applications like imaging, drug delivery and targeting since they have been reported to help to improve drug solubility, release and bioavailability [17]. Silica-gold nanoparticles can also be used in catalysis for chemical reactions such as catalytic hydrogenation and oxidation [18], in electronics for the development of electronic devices such as solar cells and sensors [19], sensing devices for various analytes such as proteins, DNA and small molecules [20].

Different methods have been used to deposit gold nanoparticles into silica supports. The most common methods include modification of the mesoporous silica support using various organic functional groups through co-condensation technique before gold can be loaded or through post grafting [21, 22], chemical vapor deposition through the usage of expensive organometallic gold precursors [23] and one-pot synthesis through incorporating gold and a coupling agent which contains functional groups [24]. Huerta et al. [25] used supercritical CO_2 modified with ethanol and also wet impregnation method to deposit gold nanoparticles on SBA-15. Bore et al. [26] used a thermal sintering method where gold nanoparticles were sintered on mesoporous silica MCM-41 at high temperatures. Usually a surfactant is used when nanoparticles are loaded into a silica support. The removal of the template is very crucial when it comes to supported metal nanoparticles since the template plays a huge role in terms of particle size, morphology and particle distribution [27]. Several methods of template removal have been investigated by researchers such as calcining the silica-gold nanoparticles at

high temperatures (500 °C and above) [2, 26], solvent extraction using hydrochloric acid (HCl) and methanol [13, 28] and also sonication at 40 °C using ethanol and HCl [29].

The major drawbacks of the deposition methods reported in literature are the utilization of toxic materials that are harmful to the environment which can lead to ground water contamination and thehigh temperature and pressure techniques that are used in some of these deposition methods are not safe or energy efficient. The disadvantage of the methods that utilize templates or surfactants during the synthesis is that these methods need to employ certain strategies to remove the surfactants and these are not eco-friendly since they involve high temperatures or the usage of mineral acids such as hydrochloric acid to facilitate solvent extraction.

Waste valorization is an important aspect in enhancing economic sustainability and minimizing the environmental impact. Sugarcane leaves are a waste from the sugar industry and are usually burnt before harvest which produces crystalline silica polymorphs (cristobalite or quartz) which in 1997 was classified as a human carcinogen by the international agency for research on cancer (IARC) [30]. Inhaling crystalline silica during or after the burning of sugarcane leaves has also been reported to cause life threatening health issues such as shortness of breath, aggravation of certain pre-existing conditions such as asthma and even cause lung cancer [31, 32]. This study reports different methods that were used to deposit gold nanoparticles on a silica xerogel support that was synthesized from sugarcane leaves through a sol-gel method. The reported study was conducted at a maximum temperature of 80 °C under atmospheric pressure and did not use mineral acids. The gold nanoparticles were deposited using two different techniques: (i) nanoparticles were synthesized separately and then added in a sodium silicate solution and (ii) the nanoparticles were synthesized in-situ (within the sodium silicate solution) and both samples were converted into silica/gold nanoparticles (Si/AuNPs) xerogel. The silica/AuNPs that have been synthesized this way have an advantage since they are easy to handle and a desired slice with specific thickness can be cut mechanically to alter the level of adsorption. Alternatively, our produced product can be grounded to fine powder and used as desired. To the best of our knowledge, no work has been reported in the literature which focused on the usage of biogenic silica from sugarcane leaves as a support for gold nanoparticles through a sol gel method.

2 Materials and method

2.1 Materials

Gold (III) chloride trihydrate (99.9+ %), sodium borohydride, Polyvinyl alcohol (average molecular weight, 9000–10,000), sodium hydroxide and citric acid were all bought from Sigma Aldrich, South Africa. Absolute ethanol (99,9 AR) was bought from Reflecta laboratory supplies (South Africa) and sugarcane leaves were obtained from sugarcane farmers in Verulam, South Africa. All chemicals were used as received.

2.2 Methods

2.2.1 Sodium silicate preparation

Sodium silicate was prepared by dissolving 16 g of biogenic silica (which was previously prepared through a method reported by Maseko et al. [33]) in 800 mL of sodium hydroxide and the mixture was refluxed for 2 h at 80 °C with continuous stirring. After 2 h, the reaction was terminated and the mixture cooled to room temperature and later gravity filtered to remove any impurities.

2.2.2 Deposition of gold into the biogenic silica support

Si/AuNPs with gold loading of 2 wt% were prepared through a sol-gel method. In a 500 ml beaker, 200 ml of sodium silicate was added. Roughly 80 ml of 1 M citric acid was added to this mixture with continuous stirring to bring the pH to about 9.5. Once the pH reached 9.5, 2 wt% of 0.01 M gold (III) chloride trihydrate and 1 wt% PVP were added to the sodium silicate solution and the resulting mixture was continuously stirred for 30 min. After 30 min, 2 ml of cold 0.1 M sodium borohydride was added to the mixture followed with vigorous stirring for a further 30 min as the mixture gradually turned into a purple color. After 30 min, the stirring was stopped and 1 M citric acid was added dropwise to the Au-Si solution until a pH of 8.7 was reached and this is the pH value where a sol started to form. The sol was stirred for a further minute and instantly transformed into a purple gel. The gel was covered with a parafilm and left in a fume hood to age for a period of 8 h at room temperature. The resulting gel was later washed and subjected to a solvent exchange method as reported by Maseko et al. [34]. After solvent exchange, the surfactant removal was conducted as per the method reported by Jabariyan et al. [29] except that in this study HCl was substituted with citric acid. The Si/AuNPs partially dried gel were subsequently dried at 80 °C for 24 h in an oven. The sample was later removed from the oven, grounded with pestle and mortar and labeled *Si/AuNPs-Insitu* before being stored in an air-tight container and kept in a desiccator for analysis. Another synthesis was conducted where gold nanoparticles were synthesized using a method reported by Hou et al. [35]. About 200 mL of sodium silicate solution was hydrolyzed by 1 M citric acid until a pH of 9.5, where a pink solution of 2 wt% of the synthesized gold nanoparticles were added while the solution was continuously stirred. Citric acid was further added until a pH of 8.7 was

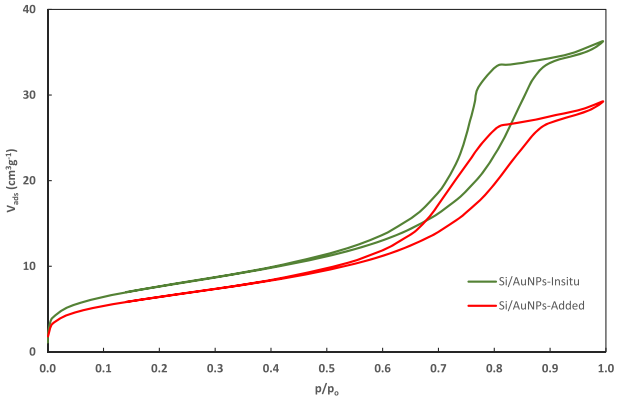

Fig. 1 Nitrogen adsorption-desorption isotherms of the two Si/Au nanoparticles samples

reached. The aging, washing and further steps were followed exactly as in the Si/AuNPs-Insitu synthesis. The dried product was grounded using pestle and mortar due to its solid structure and stored in an air-tight container, labeled *Si/AuNPs-Added* and kept in a desiccator for analysis.

2.3 Characterization

The UV-Visible measurements were obtained through a PerkinElmer LAMBDA 25 (Waltham, MA, USA). FTIR spectra were achieved through the usage of a Nicolet Avatar 360 FTIR spectrometer (Madison, WI, USA), where 32 scans in the range of 4000–400 cm^{-1} were taken per sample. Nitrogen adsorption-desorption measurement were conducted using Micrometrics ASAP 2010 (Norcross, GA, USA), the samples were initially degassed at 250 °C for 12 h to remove any absorbed water molecules. The X-ray fluorescence was performed to measure chemical analysis using a S4 Explorer-WDXRF Bruker (Karlsruhe, Germany). The transition electron microscopy (TEM) images were obtained from JEOL 2100 HRTEM (Japan). Energy dispersive X-ray (EDX) and scanning electron microscopy images were obtained from a Zeiss Ultra Plus FEG SEM (Oberkochen, Germany). The phase identification was measured from a Seifert XRD 7 apparatus that is equipped with Ni-149 Cu- Kα radiation ($\lambda = 1.54$ Å).

3 Results and discussion

3.1 Nitrogen adsorption-desorption

The nitrogen sorption isotherms of the Si-AuNPs samples are displayed in Fig. 1. The nitrogen uptake of both the samples is observed to be relatively small at a low relative pressure but it slowly increases as the relative pressure increases as can be observed from Fig. 1. According to Liu et al. [36], this indicates the possible presence of micropores within the pore structure of the Si-Au samples. Both samples displayed a type IV isotherm which is a trait of mesoporous materials [37]. The observed hysteresis loops have a moderately higher closure point situated at a relative pressure of 0.5 and they can be classified as H2. The H2-Type is known to be affiliated with ink-bottle type of pores and also interconnected pore networks that consists of different sizes and shapes [25]. The presence of the hysteresis loop implies the existence of larger mesopores [38]. There is no saturation that took place at relative pressures close to unity and this implies that both mesopores and macropores with a wide size distribution are present in the samples [39].

Metal doping is known to significantly alter the specific surface area of a metal support as a result of the formation of nanoparticles clusters within the silica support [40]. A number of researchers have reported a significant decrease of more than 50% after nanoparticles were incorporated within the silica support. Liu et al. [36] deposited palladium nanoparticles on a rice husk derived support and their surface area decreased by 52%. A whooping decrease in surface area of 95% was reported by Thabet et al. [41] when they deposited titanium nanoparticles on a rice husk derived support. Zhu et al. [42] deposited gold nanoparticles on SBA-15 mesoporous silica and after deposition, their BET surface area decreased by 78%. In this study, the BET surface area of Si/AuNPs -Insitu and Si/AuNPs-Added produced were found to be 619 m^2g^{-1} and 322 m^2g^{-1}, respectively. Both of these specific surface areas are lower than the specific surface area for silica without deposited gold nanoparticles which is 668 m^2g^{-1} as expected due to the trend from the literature. Incorporating gold nanoparticles into the silica support slightly reduced the specific surface area by 7% for Si/Au-insitu, however, the specific surface area for Si/Au-added sample was significantly reduced by 52% due to the deposited agglomerated nanoparticles [7, 41]. Ray et al. [43] mentioned that the size and position of the deposited nanoparticles have an effect on the specific surface area of the loaded metal. According to these authors, the smaller the nanoparticles within the metal, the least the decrease in the BET surface area, provided the nanoparticles strictly deposited within the pores. The pore diameter for Si/Au-insitu and Si/Au-added was observed to be 8.3 and 11.1 nm, respectively. The pore diameters of both the Si/NPs are slightly higher than that of the silica without deposited nanoparticles as displayed in Table 1. This could be due to the nanoparticles position within the silica support. The deposition of gold nanoparticles in smaller mesopores results in a shift of the pore size distribution of the remaining pores to larger pores, but this effect is mainly observed if silica supports are loaded with preformed nanoparticles or other impregnation procedures. According to Chen et al. [44] and Wu et al. [5], if some of the deposited nanoparticles implant on the silica walls instead of the pores this could cause void defects or micropores within the silica after the removal of the surface modifier

(usually an organic group) and sequentially result in higher pore diameter. The method reported in this study used a similar approach where ethanol was introduced into the Si/AuNPs gel to gradually replace the water molecules so that when the ethanol is evaporated a void is created within the silica. The pore volume of Si/Au-Insitu was 1.28 cm^3g^{-1} while that of Si/Au-Added was 0.98 cm^3g^{-1}. The pore size distribution according to the BJH-method (Barrett-Joyner-Halenda) [45] is presented in Fig. 2. The reported pore sizes were attained from the peak positions of the distribution curves. The pore size distribution demonstrates that for both the as synthesized Si/AuNPs, the majority of the pores are within the lower mesopore region. For both the Si/AuNPs, the deposition of gold nanoparticles within the biogenic silica support did reduce the porous properties of the Si/AuNPs. However, the produced samples still had good properties of the pore system. This can be attributed to successful solvent exchange and also removal of the surfactant through the sonication method reported by Jabariyan et al. [29].

Table 1 Textural properties of bare silica and silica with deposited gold nanoparticles obtained by nitrogen sorption analysis

Au-Silica nanoparticle samples	A_{BET} (m^2g^{-1})	Pore Diameter (nm)	Pore Volume (cm^3g^{-1})	Au Particle size (nm) (TEM)
Si-PVA	668	7.5	1.26	–
Au/Si-Insitu	619	8.3	1.28	4.1
Au/Si-Added	322	11.1	0.90	2.8

3.2 UV-Vis spectroscopy

Optical absorption spectra for gold nanoparticles and that of both of the Si/AuNPs samples are shown in Fig. 3. The plasmon absorption is highly dependent on the particle shape, size and dielectric medium [46]. The UV-Vis spectrum of gold nanoparticles has a typical surface plasmon resonance (SPR) band at 524 nm. However, the spectra of both of the gold loaded silica supports show a red shifted SPR band at 545 nm which indicates the existence of gold nanoparticles within the mesoporous silica support [47]. Supported AuNPs are known to have absorption profiles that are broader and tend to shift to blue or red based on the polarization of the external field [48]. According to Ghosh and Pal [49] and Budnyk [50], the observed red shift is due to the small gold nanoparticles

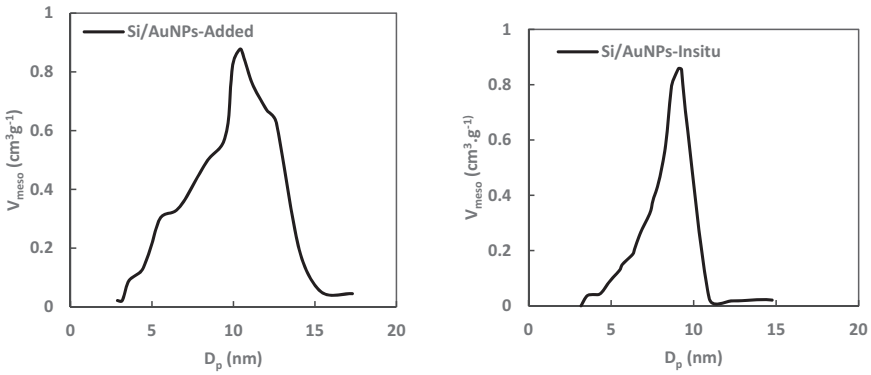

Fig. 2 Pore size distribution of silica samples with deposited gold nanoparticles

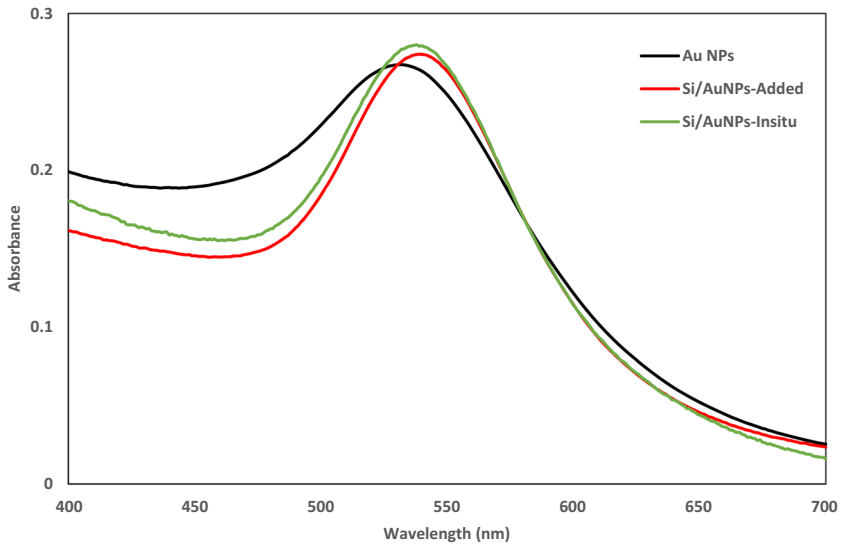

Fig. 3 UV-VIS spectra of gold nanoparticles and Si/AuNPs samples

forming clusters of different structures, orientations and sizes or structures that are densely packed and cause electronic coupling of single gold particles to each other within the silica support. This can be corroborated by SEM and TEM results below (Figs. 5 and 6, respectively) which indicate an aggregation of small nanoparticles.

3.3 X-ray fluorescence (XRF) and EDX analysis

The chemical composition of silica/gold nanoparticles samples was conducted through an XRF analysis and the results are displayed in Table 2. In both samples, 2 wt% of gold metal was loaded during the synthesis. Both the samples demonstrate gold being present in them, however, the composition at which it is present is not the same. The sample that had the gold nanoparticles synthesized insitu have a composition of 1.98 wt% (0.02 wt% less than the gold added). When it comes to the sample where gold nanoparticles were prepared separately and then added into a sodium silicate solution, almost 50% of the gold loaded on this solution was lost. It is worth noting that during the washing of the gel, the waste solution for this sample was primarily pink/purple while for the insitu synthesis the waste was colorless. It is reasonable to assume that most of the nanoparticles were lost during the gel washing. Other impurities such as Na_2O, CaO and K_2O are also present in both the Si/AuNPs samples at very low concentrations as demonstrated in Table 2.

Table 2 Chemical analysis of silica/AuNPs- Insitu and silica/Au NPs-Added

Constituent	Si/AuNPs-Insitu (wt %)	Si/AuNPs-Added (wt %)
SiO_2	97.95	98.92
Na_2O	0.04	0.03
Au	1.98	1.01
CaO	0.02	0.02
K_2O	0.01	0.02

EDX measurements were also conducted to identify the elemental composition in the produced Si/AuNPs samples, the results are presented in Fig. 4. It can be seen that silica was the main inorganic constituent in both samples as expected. Gold was also detected in both the samples, however, the sample with gold nanoparticles prepared insitu

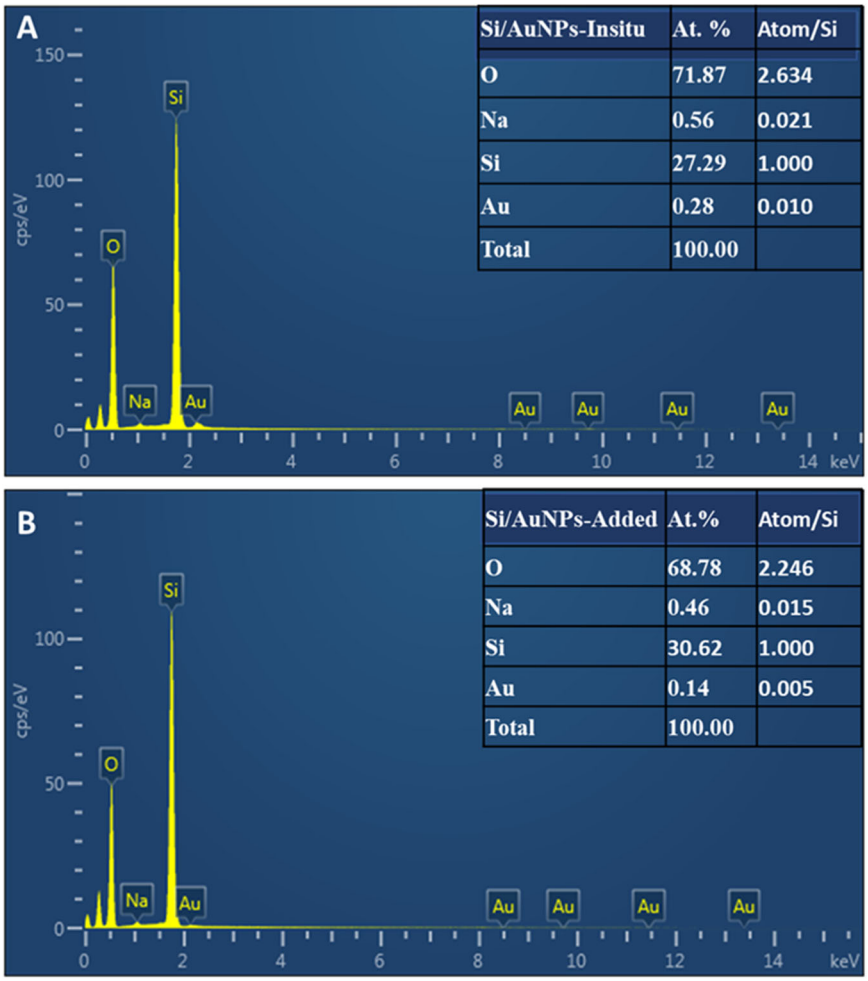

Fig. 4 EDX Images for **A** Si/AuNPs- Insitu and **B** Si/AuNPs-Added

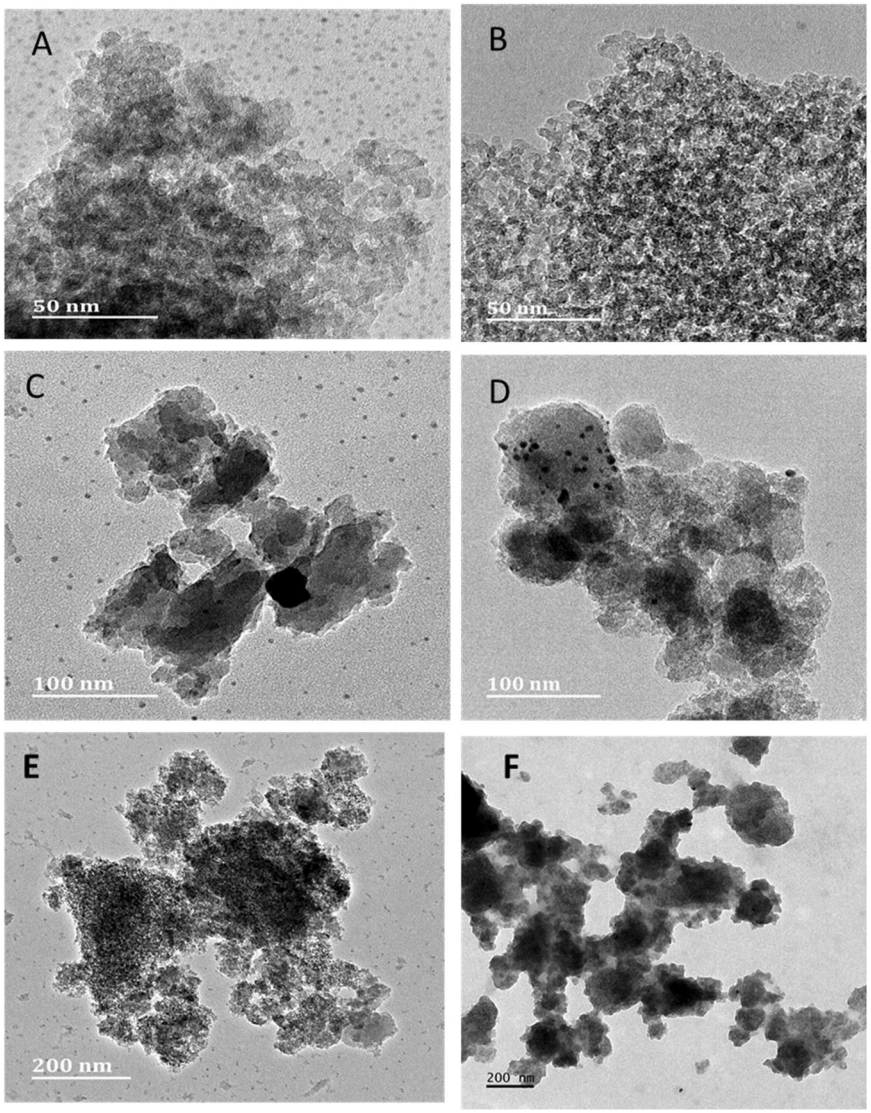

Fig. 5 TEM images of gold nanoparticles deposited on a silica support(**5A**), **5C** and **5E**: Si/AuNPs-Added, **5B**, **5D** and **5F**: Si/AuNPs-Insitu

had more gold present than the sample where gold nanoparticles were synthesized separately. This corroborates the results obtained from XRF in Table 2.

3.4 Transmission electron microscopy

TEM was used to study the particle size, distribution and shape of the produced nanoparticles. The TEM images of Si/AuNPs samples were observed to differ in terms of gold nanoparticles positioning based on the synthesis method. Gold nanoparticles in both Si/AuNPs samples are fundamentally spherical in nature with most particles combined to form larger particles which led to significant agglomeration. The gold nanoparticles that were synthesized insitu seem to have deposited/imbedded within the silica network, there is no AuNPs that is sighted out of the support as demonstrated in Fig. 5B, D and F. However, the gold nanoparticles that were synthesized separately and then added to the sodium silicate solution seem to have not incorporated into the silica network that much, instead they are scattered outside with a few nanoparticles within the silica network as observed in Fig. 5A, C and E. The gold nanoparticles on Si/AuNPs-Added sample were found to be smaller (average of 2.8 nm) while the Si/AuNPs-Insitu were slightly bigger (average of 4.1 nm) as can be seen in Table 1. In both of the samples, the AuNPs are unevenly distributed and also were subjected to major agglomeration. Silica nanoparticles also are seen to have agglomerated and formed larger particles which resulted in mesopores as observed in nitrogen adsorption-desorption isotherm.

3.5 Scanning electron microscopy

SEM was used to investigate the surface morphology and also the general morphological features of the prepared Si/AuNPs samples. Figure 6A, C show Si/AuNPs-Added

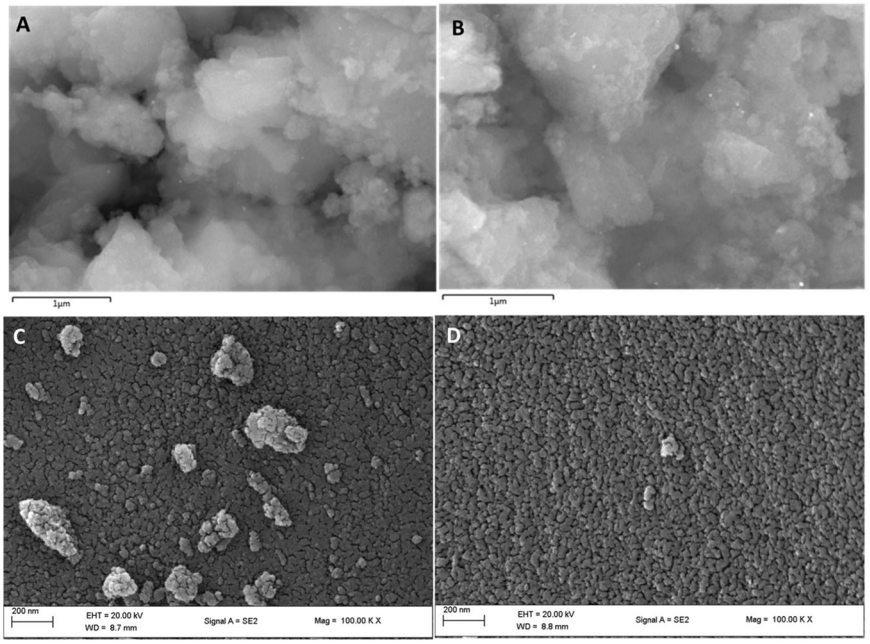

Fig. 6 SEM images of gold nanoparticles deposited on a silica support (Fig. **6A** and **C** sample Si/AuNPs-Added, Fig. **6B** and **D** sample Si/AuNPs-Insitu)

while Fig. 6B, D show Si/AuNPs-Insitu. Both Fig. 6C, D demonstrate silica supports with non-uniform particle shapes and sizes with visible macropores even after the deposition of gold nanoparticles. Figure 6A, B show scattered gold nanoparticles within the surfaces which are white in color, however these nanoparticles are larger in size than the ones detected via TEM (Fig. 5) since they could be identified by SEM. This implies that the nanoparticles produced had different sizes. The gold nanoparticles seem to be more populated in the silica gold nanoparticles sample that was synthesized insitu which agrees with the XRF results which reported that the gold loading in the Si/AuNPs-Insitu sample was more than the Si/AuNPs-Added sample.

4 Conclusions

The deposition of gold nanoparticles within the sugarcane derived biogenic silica support using two deposition methods: synthesizing nanoparticles insitu and also synthesizing nanoparticles separately and add them to a sodium silicate solution to form the individual silica/gold nanoparticles samples was studied. Both methods resulted in agglomerated silica and gold particles and gold nanoparticles synthesized in-situ were deposited within the silica support while for the nanoparticles that were synthesized separately most of the gold nanoparticles did not deposit within the silica network and hence reducing the resulting gold loading percentage within the product. The in-situ synthesis method of gold nanoparticles proved to be a better method since it retained the original metal loading while the other method resulted in silica with almost half of the gold metal loading. Both produced silica gold nanoparticles samples had BET surface areas lower than that of silica without nanoparticles deposited in them with the Si/AuNPs-Insitu sample having significantly higher specific surface area of 619 m^2g^{-1} than 322 m^2g^{-1} for Si/AuNPs-Added. The agglomeration of silica particles prevented most of the gold nanoparticles to successfully deposit within the support for both methods of synthesis. The deposition of the nanoparticles within the biogenic silica support caused the surface plasmon resonance of silica/gold nanoparticles to be red shifted. Both methods produced silica/gold nanoparticles that had small mesopores and additional macropores. The intendent study of using this material as a catalyst will focus on employing the S/AuNPs-Insitu method since it retained the deposited gold nanoparticles.

Funding Open access funding provided by University of KwaZulu-Natal.

Compliance with ethical standards

Conflict of interest The authors declare no competing interests.

Publisher's note Springer Nature remains neutral with regard to jurisdictional claims in published maps and institutional affiliations.

References

1. Lopez-Sanchez JA et al. (2008) Au–Pd supported nanocrystals prepared by a sol immobilisation technique as catalysts for selective chemical synthesis. Phys Chem Chem Phys 10:1921–1930. https://doi.org/10.1039/b719345a
2. Li Y et al. (2015) Synthesis of gold nanoparticles on rice husk silica for catalysis applications. Ind Eng Chem Res 54:5656–5663. https://doi.org/10.1021/acs.iecr.5b00216
3. Félix LL, Porcel JM, Aragón FFH, Pacheco-Salazar DG, Sousa MH (2021) Simple synthesis of gold-decorated silica nanoparticles by in situ precipitation method with new plasmonic properties. SN Appl Sci 3:1–10. https://doi.org/10.1007/s42452-021-04456-0
4. Chen L, Hu J, Qi Z, Fang Y, Richards R (2011) Gold nanoparticles intercalated into the walls of mesoporous silica as a versatile redox catalyst. Ind Eng Chem Res 50:3642–13649. https://doi.org/10.1021/ie200606t
5. Wu P, Bai P, Lei Z, Loh KP, Zhao XS (2011) Gold nanoparticles supported on functionalized mesoporous silica for selective oxidation of cyclohexane. Microporous Mesoporous Mater 141:222–230. https://doi.org/10.1016/j.micromeso.2010.11.011
6. Min BK, Friend CM (2007) Heterogeneous gold-based catalysis for green chemistry: Low-temperature CO oxidation and propene oxidation. Chem Rev 107:2709–2724. https://doi.org/10.1021/cr050954d
7. Velpula VRK, Peesapati S, Enumula SS, Burri DR, Ketike T, Narani A (2020) Biomass waste rice husk derived silica supported palladium nanoparticles: an efficient catalyst for Suzuki–Miyaura and Heck–Mizoroki cross-coupling reactions. SN Appl Sci 2:1–12. https://doi.org/10.1007/s42452-020-03920-7
8. Jin Y et al. (2009) Amorphous silica nanohybrids: Synthesis, properties and applications. Coord Chem Rev 253(23–24): 2998–3014
9. Watermann A, Brieger J (2017) Mesoporous silica nanoparticles as drug delivery vehicles in cancer. Nanomaterials 7(189):1–17. https://doi.org/10.3390/nano7070189
10. Chiang W-S, Fratini E, Baglioni P, Chen J-H, Liu Y (2016) Pore size effect on methane adsorption in mesoporous silica materials studied by small-angle neutron scattering. Am Chem Soc 32(35):8849–8857. https://doi.org/10.1021/acs.langmuir.6b02291
11. Castillo RR, Baezaa A, Vallet-Regí M (2017) Recent applications of the combination of mesoporous silica nanoparticles with nucleic acids: development of bioresponsive devices, carriers and sensors. Biomater Sci 5:353–377. https://doi.org/10.1039/C6BM00872K
12. Verho O, Zheng H, Gustafson KPJ, Nagendiran A, Zou X, and Bäckvall JE. Application of Pd nanoparticles supported on mesoporous hollow silica nanospheres for the efficient and selective semihydrogenation of alkynes. ChemCatChem. 8, 2016, https://doi.org/10.1002/cctc.201501112.
13. Wubetu YS et al. Particle size control of monodispersed spherical nanoparticles with MCM-48-type mesostructure via novel rapid synthesis procedure. J Nanoparticle Res. 21, 2019, https://doi.org/10.1007/s11051-019-4699-7.
14. Kuśtrowski P, Chmielarz L, Dziembaj R, Cool P, Vansant EF (2005) Modification of MCM-48-, SBA-15-, MCF-, and MSU-type mesoporous silicas with transition metal oxides using the molecular designed dispersion method. J Phys Chem B 109:11552–11558. https://doi.org/10.1021/jp050696o
15. Verho O et al. (2014) Mesoporous silica nanoparticles applied as a support for Pd and Au nanocatalysts in cycloisomerization reactions. APL Mater 2:113316. https://doi.org/10.1063/1.4901293
16. Wang Y et al. (2014) The investigation of MCM-48-type and MCM-41-type mesoporous silica as oral solid dispersion carriers for water insoluble cilostazol. Drug Dev Ind Pharm 40:8 1 9–8 2 8. https://doi.org/10.3109/03639045.2013.788013
17. Shilpi S, Khatri K (2016) Gold nanoparticles as carrier(s) for drug targeting and imaging. Female Leadersh Chall J 3(3):154–170. https://doi.org/10.2174/2211738504666151127192830
18. Chen H, Li Z, Qin Z, Kim HJ, Abroshan H, Li G (2019) Silica-encapsulated gold nanoclusters for efficient acetylene hydrogenation to ethylene. ACS Appl Nano Mater 2(5):2999–3006. https://doi.org/10.1021/acsanm.9b00384
19. Kim G-H, Ramesh S, Kim J-H, Jung D, Kim HS (2014) Cellulose-silica/gold nanomaterials for electronic applications. J Nanosci Nanotechnol 14(10):7495–7501. https://doi.org/10.1166/jnn.2014.9551
20. Saha K, Agasti SS, Kim C, Li X, Rotello VM (2012) Gold nanoparticles in chemical and biological sensing. Chem Rev 112(5):2739–2779. https://doi.org/10.1021/cr2001178
21. Yang CM, Liu PH, Ho YF, Chiu CY, Chao KJ (2003) Highly dispersed metal nanoparticles in functionalized SBA-15. Chem Mater 15(1):275–280. https://doi.org/10.1021/cm020822q
22. Guari Y et al. (2003) In situ formation of gold nanoparticles within thiol functionalized HMS-C16 and SBA-15 type materials via an organometallic two-step approach. Chem Mater 15(10):2017–2024. https://doi.org/10.1021/cm0213218
23. Mitsutaka O, Susumu T, Masakazu I, Masatake H (1998) Chemical vapor deposition of gold nanoparticles on MCM-41 and their catalytic activities for the low-temperature oxidation of CO and of H2. Chem Lett 27(4):315–316. https://doi.org/10.1246/cl.1998.315
24. Zhu H, Lee B, Dai S, Overbury SH (2003) Coassembly synthesis of ordered mesoporous silica materials containing au nanoparticles. Langmuir 19:3974–3980. https://doi.org/10.1021/la027029w
25. Huerta A et al. Deposition of Au nanoparticles into mesoporous SiO2 SBA-15. J Supercrit Fluids. 184, 2022, https://doi.org/10.1016/j.supflu.2022.105582.
26. Bore MT, Pham HN, Switzer EE, Ward TL, Fukuoka A, Datye AK (2005) The role of pore size and structure on the thermal stability of gold nanoparticles within mesoporous silica. J Phys Chem 109:2873–2880. https://doi.org/10.1021/jp045917p
27. Alijani S et al. (2020) Capping agent effect on pd-supported nanoparticles in the hydrogenation of furfural. Catalysts 10(1):1–16. https://doi.org/10.3390/catal10010011
28. Ghosh A, Patra CR, Mukherjee P, Sastry M, Kumar R (2003) Preparation and stabilization of gold nanoparticles formed by in situ reduction of aqueous chloroaurate ions within surface-modified mesoporous silica. Microporous Mesoporous Mater 58(3):201–211. https://doi.org/10.1016/S1387-1811(02)00626-1
29. Jabariyan S, Zanjanchi MA (2012) A simple and fast sonication procedure to remove surfactant templates from mesoporous MCM-41. Ultrason Sonochem 19:1087–1093. https://doi.org/10.1016/j.ultsonch.2012.01.012
30. Sato T, Shimosato T, Klinman DM (2018) Silicosis and lung cancer: current perspectives. Lung Cancer 9:91–101. https://doi.org/10.2147/LCTT.S156376
31. Blond JSL, Horwell CJ, Williamson BJ, Oppenheimer C (2010) Generation of crystalline silica from sugarcaneburning. J Environ Monit 12(7):1459–1470. https://doi.org/10.1039/C0EM00020E
32. Poinen-Rughooputh S, Rughooputh MS, Guo Y, Rong Y, and Chen W (2016) Occupational exposure to silica dust and risk of

lung cancer: an updated meta-analysis of epidemiological studies. BMC Public Health. 16, https://doi.org/10.1186/s12889-016-3791-5.
33. Maseko NN et al. (2021) The production of biogenic silica from different South African agricultural residues through a thermochemical treatment method. Sustainability 13(577):1–14. https://doi.org/10.3390/su13020577
34. Maseko NN, Enke D, Iwarere SA, Oluwafemi OS, and Pocock J (2023) Synthesis of low density and high purity silica xerogels from South African sugarcane leaves without the usage of a surfactant. Sustainability. 15, https://doi.org/10.3390/su15054626.
35. Hou W, Dehm NA, Scott RWJ (2008) Alcohol oxidations in aqueous solutions using Au, Pd, and bimetallic AuPd nanoparticle catalysts. J Catal 253:22–27. https://doi.org/10.1016/j.jcat.2007.10.025
36. Liu D et al. (2019) Rice husk derived porous silica as support for Pd and CeO2 for low temperature catalytic methane combustion. Catalysts. https://doi.org/10.3390/catal9010026.
37. Xu Y et al. (2020) Mesoporous silica supported orderly-spaced gold nanoparticles SERS-based sensor for pesticides detection in food. Food Chem 315:126300. https://doi.org/10.1016/j.foodchem.2020.126300
38. Alyosef HA et al. (2015) Meso/macroporous silica from miscanthus, cereal remnant pellets, and wheat straw. ACS Sustain Chem Eng 3(9):2012–2021. https://doi.org/10.1021/acssuschemeng.5b00275
39. Kumar R, Bhattacharjee B (2003) Porosity, pore size distribution and in situ strength of concrete. Cem Concr Res 33(1):155–164. https://doi.org/10.1016/S0008-8846(02)00942-0
40. Silva AGM et al. (2013) Gold, palladium and gold–palladium supported on silica catalysts prepared by sol–gel method: synthesis, characterization and catalytic behavior in the ethanol steam reforming. J Sol-Gel Sci Technol 67:273–281. https://doi.org/10.1007/s10971-013-3076-8
41. Thabet A, Basheer C, HtunMaung T, Al-Muallem HA, Kalanthoden AN (2015) Rice husk supported catalysts for degradation of chlorobenzenes in capillary microreactor. J Nanomaterials 215:1–9. https://doi.org/10.1155/2015/912036
42. Zhu K, Hu J, Richards R (2005) Aerobic oxidation of cyclohexane by gold nanoparticles immobilized upon mesoporous silica. Catal Lett Vol 100:195–199. https://doi.org/10.1007/s10562-004-3454-5
43. Ray S, Biswas R, Banerjee R, Biswas P (2020) A gold nanoparticle intercalated mesoporous silica based nanozyme for selective colorimetric detection of dopamine. Nanoscale Adv 2(2):734–745. https://doi.org/10.1039/C9NA00508K
44. Chen L, Hu J, Richards R (2009) Intercalation of aggregation-free and well-dispersed gold nanoparticles into the walls of mesoporous silica as a robust "green" catalyst for n-alkane oxidation. J Am Chem Soc 131(3):914–915. https://doi.org/10.1021/ja808860v
45. Barrett EP, Joyner LG, Halenda PP (1951) The determination of pore volume and area distributions in porous substances. I. computations from nitrogen isotherms. J Am Chem Soc 73:373–380. https://doi.org/10.1021/ja01145a126
46. Niculescu V-C (2020) Mesoporous silica nanoparticles for bioapplications. Front Mater 7(36):1–14. https://doi.org/10.3389/fmats.2020.00036
47. Trayford C et al. (2022) Mesoporous silica-coated gold nanoparticles for multimodal imaging and reactive oxygen species sensing of stem cells. ACS Appl Nano Mater 5(3):3237–3251. https://doi.org/10.1021/acsanm.1c03640
48. Elahi N, Kamali M, Baghersad MH (2018) Recent biomedical applications of gold nanoparticles: a review. Talanta 184:537–556. https://doi.org/10.1016/j.talanta.2018.02.088
49. Ghosh SK, Pal T (2007) Interparticle coupling effect on the surface plasmon resonance of gold nanoparticles: from theory to applications. Chem Rev 107(11):4797–4862. https://doi.org/10.1021/cr0680282
50. Budnyk AP, Cherkasovaa SO, Damin A (2017) One-pot sol-gel synthesis of porous silica glass with gold nanoparticles. Mendeleev Commun 27(5):531–534. https://doi.org/10.1016/j.mencom.2017.09.035